CellPress

The Polyketide Synthase Pks13 Catalyzes a Novel Mechanism of Lipid Transfer in Mycobacteria

Sabine Gavalda,[1,3,4] Fabienne Bardou,[1,3,4] Françoise Laval,[1,3] Cécile Bon,[2,3] Wladimir Malaga,[1,3] Christian Chalut,[1,3] Christophe Guilhot,[1,3] Lionel Mourey,[2,3] Mamadou Daffé,[1,3] and Annaïk Quémard[1,3,*]
[1]Department Tuberculose & Biologie des Infections
[2]Department Biologie Structurale et Biophysique
CNRS, IPBS (Institut de Pharmacologie et de Biologie Structurale), UMR5089, 205 route de Narbonne, BP64182, 31077 Toulouse, France
[3]Université de Toulouse, UPS, IPBS, 31077 Toulouse, France
[4]Co-first author
*Correspondence: annaik.quemard@ipbs.fr
http://dx.doi.org/10.1016/j.chembiol.2014.10.011

SUMMARY

Mycolate-containing compounds constitute major strategic elements of the protective coat surrounding the tubercle bacillus. We have previously shown that FAAL32-Pks13 polyketide synthase catalyzes the condensation reaction, which produces α-alkyl β-ketoacids, direct precursors of mycolic acids. In contrast to the current biosynthesis model, we show here that Pks13 catalyzes itself the release of the neosynthesized products and demonstrate that this function is carried by its thioesterase-like domain. Most importantly, in agreement with the prediction of a trehalose-binding pocket in its catalytic site, this domain exhibits an acyltransferase activity and transfers Pks13's products onto an acceptor molecule, mainly trehalose, leading to the formation of the trehalose monomycolate precursor. Thus, this work allows elucidation of the hinge step of the mycolate-containing compound biosynthesis pathway. Above all, it highlights a unique mechanism of transfer of polyketide synthase products in mycobacteria, which is distinct from the conventional intervention of the discrete polyketide-associated protein (Pap)-type acyltransferases.

INTRODUCTION

Tuberculosis (TB) represents a major public health problem worldwide. This disease remains today one of the leading causes of death from an infectious agent. Nearly nine million people fell ill and 1.3 million died from TB in 2012 (WHO, 2013). Drug-sensitive TB can be cured with a standard 6-month therapy. However, the emergence of multidrug-resistant and extensively drug-resistant *Mycobacterium tuberculosis* strains has challenged TB control. Therefore, the discovery of novel pharmacological targets for the development of a new generation of drugs is urgently needed.

The very thick envelope of *Mycobacterium tuberculosis* and other pathogenic mycobacteria is characterized by a broad array of exotic complex lipids that are key players in the infectious process (Daffé et al., 2014; Jackson et al., 2007). Mycolic acids are α-branched and β-hydroxylated fatty acids of exceptional chain length (e.g., C_{60}-C_{90} in *Mycobacterium*, C_{22}-C_{36} in *Corynebacterium*) that typify the *Corynebacteriales* order (Marrakchi et al., 2014). They constitute the major components of the outer membrane (mycomembrane) and are therefore determining factors in the permeability of the envelope (Gebhardt et al., 2007). The vast majority of the mycolic acids esterify the pentaarabinosyl ends of the arabinogalactan forming the cell wall mycolyl-arabinogalactan-peptidoglycan (mAGP) complex. The latter would bind to the human natural killer (NK) cell natural cytotoxicity receptor NKp44, playing a potential role in maintaining NK cell activation (Esin et al., 2013). The remaining mycolic acids form the mycolate-containing lipids composed of one or two mycolyl chains linked to the 6 and 6′ positions of trehalose and more scarcely to glucose or glycerol. These lipids constitute major determinants of the pathologies caused by the mycobacteria, acting either as proinflammatory agents, like trehalose dimycolate (TDM) and trehalose monomycolate (TMM) (Geisel et al., 2005; Glickman, 2008), or as T cell activators via their presentation by CD1b protein, like glucose monomycolate (GMM) and glycerol monomycolate (GroMM) (Layre et al., 2009; Moody et al., 2002).

Given the significance of the mycolate-containing compounds in the dialog between the tubercle bacillus and the infected host, the identification of the different biosynthesis steps leading to their formation is a very important issue, especially for the search of novel TB drug targets. Their biosynthesis pathway ends up with the transfer of the mycoloyl chains from TMM onto a polyol core (arabinogalactan, trehalose, glucose, and possibly glycerol) by the Ag85ABC mycoloyl transferase complex (Belisle et al., 1997; Jackson et al., 1999). Beforehand, the mycoloyl chains are produced by a mixed fatty acid synthase (FAS)-polyketide synthase (PKS) biosynthesis pathway, whose pivotal step is catalyzed by the FAAL32-Pks13 system (Gavalda et al., 2009; Léger et al., 2009). The discrete fatty acyl-AMP ligase FAAL32 (or FadD32) activates very long (C_{16}-C_{60}) fatty acyl chains, the "meromycoloyl chains," into AMP derivatives and loads them onto

CrossMark

Pks13 enzyme (Léger et al., 2009). The latter is a unique PKS that uses exceptionally long (C_{16}-C_{26}) extender units it condenses to the meromycolyl chains, forming α-alkyl β-ketoesters, the direct precursors of mycolic acids (see Figure S1 available online). We have deciphered the different reaction steps catalyzed by Pks13 (Gavalda et al., 2009; Léger et al., 2009). However, the mechanism of release of its products as well as the subsequent steps leading to the formation of TMM remain unknown. The acyl carrier protein (ACP) domains of the PKSs are activated by a phosphopantetheinyl (P-pant) arm that carries the growing acyl chains (e.g., Figure S1) (Walsh et al., 1997). Upon reaching its full length, the polyketide is generally released from the enzyme by the action of a thioesterase (TE) domain found at the C terminus, typically via an hydrolysis mechanism (in the case of linear molecules) or via a macrocyclisation (Hertweck, 2009). Given the high hydrophobicity of Pks13's products, the current model proposes that they would not be released as free acids in the bacterium by Pks13's own putative TE (TE_{Pks13}) domain but transferred via a discrete unknown acyltransferase (a mycoloyl transferase) onto a hydrophilic acceptor unit (Takayama et al., 2005) (Figure S1). Thus, the TE_{Pks13} domain might have a distinct role, like the function of "proofreading" generally accomplished by an external type II thioesterase (Koglin and Walsh, 2009).

The present work investigates the process of release of mycolic acid precursors from Pks13 enzyme and reveals a mechanism of transfer of PKS products during the formation of complex lipids in mycobacteria. Thus, it allows elucidation of long-sought missing pieces of the mycolate-containing compound biosynthesis pathway.

RESULTS

Pks13 Generates Polyol Derivatives

To characterize the step of release of mycolic acid precursors from Pks13, we had to perform in vitro experiments using the purified enzyme. Indeed, besides the fact that Pks13 is essential for the mycobacterial survival (Portevin et al., 2004), the blockage of one step within mycolic acid biosynthesis has proven to inactivate the complete biosynthesis pathway in the past (Vilchèze et al., 2000). For solubility and availability reasons, the condensation assays were run in the presence of the substrates naturally used by *Corynebacterium* Pks13, a radiolabeled myristic acid ([1-^{14}C]C_{14} acid) and a chemically synthesized C_{16} carboxy-acyl-CoA (carboxy-C_{16}-CoA), rather than the longer substrates found in *Mycobacterium*. The mycobacterial Pks13 enzyme was shown to be able to use these short substrates in a recombinant *Corynebacterium* strain to synthesize mycolic acids in vivo (Gavalda et al., 2009). Published data have suggested that α,α-D-trehalose or D-glucose play a role in the biosynthesis of mycolic acids (Promé et al., 1974; Puzo et al., 1979; Shimakata et al., 1986), and a more recent report has shown the requirement of trehalose (Tropis et al., 2005). In order to seek for their potential involvement during the condensation reaction catalyzed by Pks13, assays supplemented with these sugars were realized. The intact reaction media were analyzed by thin-layer chromatography (TLC). We observed the glucose- (Figure 1A, spot *c*) or trehalose-dependent (Figure 1A, spots *a* and *b*) production of radiolabeled compounds, which migrated close to the natural GMM, TMM, and TDM standards, respec-

tively. The MALDI-TOF mass spectrometry (MS) analysis of the cold condensation products was very challenging because of the very low quantity of material. Spectra of the compounds obtained in the presence of trehalose and glucose specifically displayed ion peaks expected for the mono-α-alkyl β-ketoacyl trehalose (TMM keto form or "TMM*k*") and the mono-α-alkyl β-ketoacyl glucose (GMM keto form or "GMM*k*"), respectively (Figure 1B). MALDI-TOF/TOF MS/MS analyses induced the fragmentation of these molecules and confirmed their identification (Figure S2).

Interestingly, we observed that an additional radiolabeled compound was formed when glycerol was added to the stocks of enzymes used in the condensation assays (Figure 1A, spot *d*). MALDI-TOF MS analysis revealed the presence of α-alkyl β-ketoacyl glycerol (GroMM keto form or "GroMM*k*"; Figure 1B). Moreover, in the absence of acceptor molecule in the reaction, the labeling of the most apolar compound increased (Figure 1A, spot *e*). The purified compound exhibited a behavior similar to that of the long-chain ketone standard during TLC (Figure S3A) and was identified as a C_{29} long-chain ketone by MALDI-TOF MS with a [M+H]$^+$ ion peak at *m/z* 423.35 (expected *m/z* value: 423.46). Such a compound resulted from the spontaneous decarboxylation of free α-alkyl β-ketoacid released from Pks13 by hydrolysis (Figure S3B).

These data altogether demonstrated that Pks13 generates saccharidic derivatives corresponding to trehalose mono-α-alkyl β-ketoester, the direct precursor of TMM, and to glucose mono-α-alkyl β-ketoester but also a nonsaccharidic derivative, namely glycerol mono-α-alkyl β-ketoester. The quantitative variation of condensation products was measured with respect to the initial concentration of acceptor molecule in the reaction. Significant amounts of TMM*k* were already observed at the lowest trehalose concentrations: 0.07 and 0.7 mM (Figure S4). In a general manner, increasing concentrations of a given acceptor led to a gradual increase of the quantity of the corresponding α-alkyl β-ketoacid derivative formed up to a plateau. In parallel, the labeling of the long-chain ketone deriving from the free α-alkyl β-ketoacid decreased (Figure S4). Thus, the concentration of acceptor unit available in the reaction medium determines the proportions of α-alkyl β-ketoester and α-alkyl β-ketoacid produced by Pks13. To define the preference of the enzyme between the three acceptors, competition experiments were realized. Different pairs of acceptors at equimolar concentrations were mixed in the reaction medium prior to the addition of FAAL32 and Pks13. Data showed that the predilection of Pks13 for the acceptor unit is the following: trehalose, glucose, and glycerol, in decreasing order (Figure 1C).

Pks13 Has a Narrow Acceptor Specificity

In order to establish the nature of the structural determinants that play a role in the recognition by Pks13, a series of natural analogs of glucose and trehalose (Figure 2B) was evaluated as putative acceptors of the condensation products. In the presence of 6-deoxy-D-glucose, which is devoid of hydroxyl group at position 6 where the acylation naturally occurs, no derivative could be detected by TLC (Figure 2A). D-mannose and D-allose, the epimers at positions 2 and 3 of glucose, respectively, could serve as acceptors in vitro (Figure 2A, spots *c''* and *c'''*), although with a lower efficiency than D-glucose (spot *c*) and, unexpectedly,
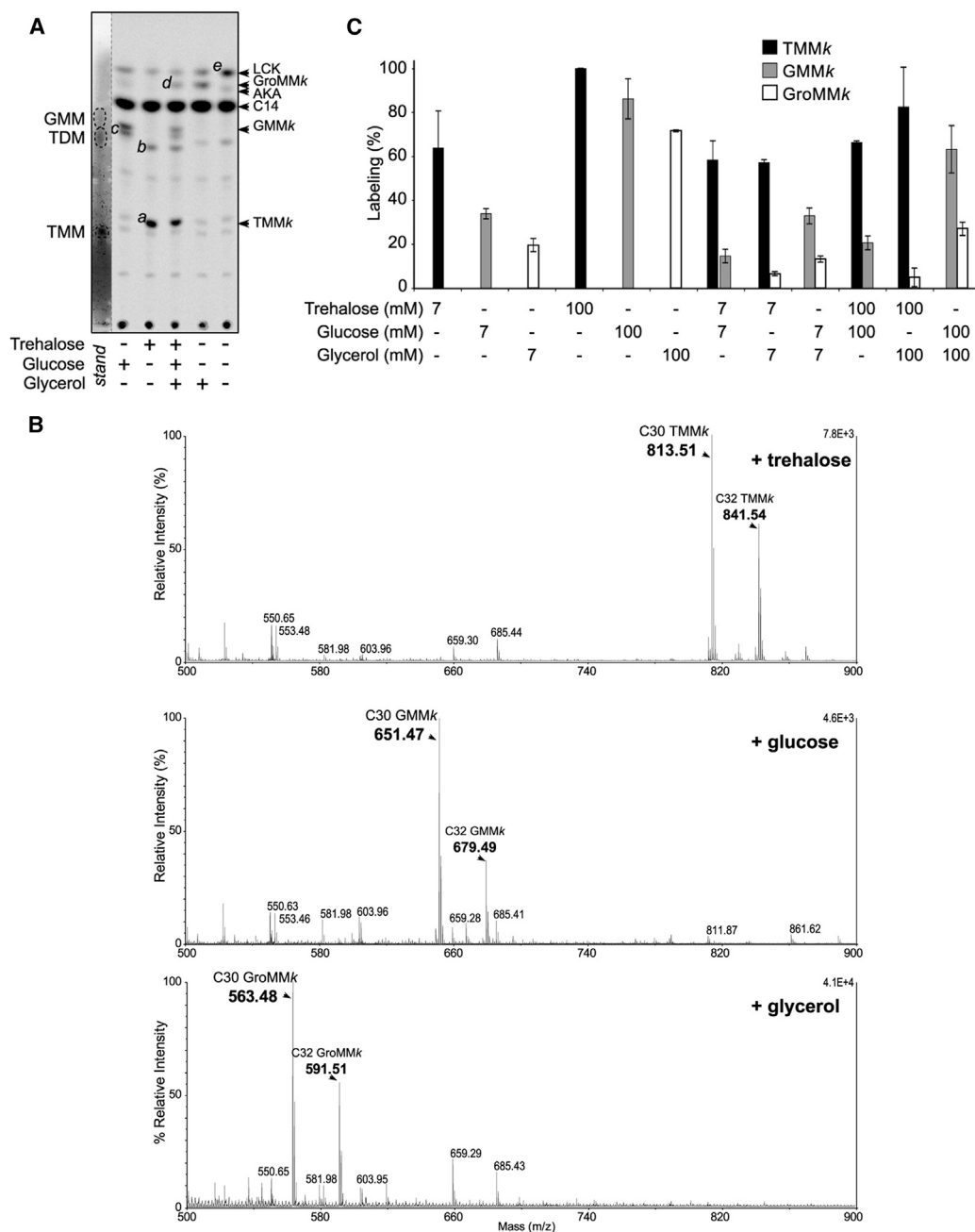
Figure 1. Formation of Different Types of α-alkyl β-ketoacid Derivative by Pks13

(A) TLC/phosphorimaging analysis of condensation assays performed in the absence (−) or in the presence (+) of 50 mM of each putative acceptor. Representative data of three independent experiments. *Stand*, standard mix of TMM, TDM, and GMM (from *C. glutamicum*) revealed by anthrone spraying. Eluent: $CHCl_3/CH_3OH/H_2O$, 65/25/4. Spots: *a*, TMM*k*; *b*, palmitoyl TMM*k* (see note below); *c*, GMM*k* (see note in Figure 2 legend); *d*, GroMM*k*; *e*, long-chain ketone (LCK). AKA: α-alkyl β-ketoacid. Note that spot *b* was identified as (α-myristyl β-ketopalmitoyl),palmitoyl trehalose by MALDI-TOF MS (monosodium adduct at *m/z*: 1051.75; theoretical *m/z* value: 1051.76); the C_{16} chain might come from the degradation of an α-alkyl β-ketoacyl chain linked to trehalose by intramolecular retro-Claisen reaction as described previously (Puzo et al., 1979). The minor radiolabeled spots are not linked to the condensation activity.

(B) MALDI-TOF MS analysis of condensation products obtained in the presence of different acceptor molecules. The assays were performed using cold carboxy-C_{16}-CoA, C_{14} acid and 100 mM acceptor molecule. The formation of C_{32} compounds, resulting from the condensation of C_{16} acid and carboxy-C_{16}-CoA, is most likely due to the fortuitous generation of C_{16} acid from carboxy-C_{16}-CoA during the assays. Theoretical *m/z* values (calculated with the Data Explorer program) of monosodium adducts: C_{30} TMM*k*, 813.53; C_{32} TMM*k*, 841.56; C_{30} GMM*k*, 651.48; C_{32} GMM*k*, 679.51; C_{30} GroMM*k*, 563.46; C_{32} GroMM*k*, 591.50.

(C) Competition experiments between trehalose, glucose, and glycerol as acceptor molecules. The biosynthesis yield of each type of α-alkyl β-ketoacid derivative, in the presence of one or two acceptor molecules at equimolar concentrations, was measured by TLC/phosphorimaging analysis. Data are means of three independent experiments ± average deviations; they are expressed as relative labelings with the points at 100 mM trehalose arbitrarily set to 100%. See also Figures S2–S4.
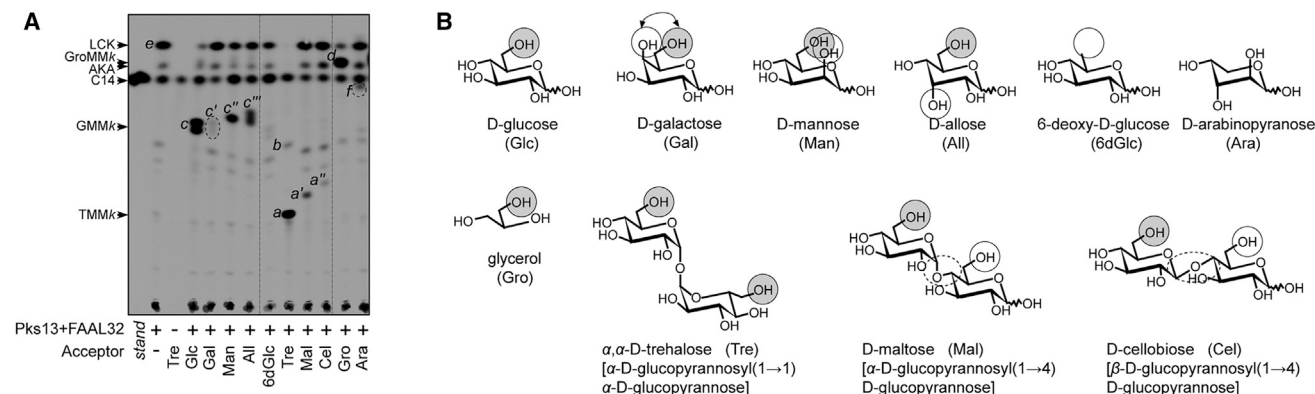
Figure 2. Analogs of Glucose and Trehalose as Putative Acceptors of Pks13's Products

(A) TLC/phosphorimaging analysis of condensation assays performed in the absence (−) or in the presence (+) of 100 mM of putative acceptor. Representative data of three independent experiments. *Stand*, standard [1-^{14}C]C$_{14}$ acid. Eluent: CHCl$_3$/CH$_3$OH/H$_2$O, 65/25/4. Spots: *a–d* and *f*, mono-α-alkyl β-ketoester of the tested polyol; *e*, long-chain ketone (LCK); AKA, α-alkyl β-ketoacid. Note that the glucose/galactose/allose α-alkyl β-ketoesters appeared as double spots (*c*, *c'*, and *c'''*, respectively) most likely because, once released in solution, the neosynthesized α-alkyl β-ketoacyl α-D-monosaccharides isomerize partially into the β tautomers. Indeed, the major forms of the corresponding free sugars in solution are the β-D-glycopyranose tautomers, whereas the mannose, whose α conformation is the major form, generated a single apparent spot (*c''*) of α-alkyl β-ketoester.

(B) Structure of tested compounds.

than glycerol (spot *d*). In the latter, the C-C bonds have no rotation constraint, which allows it to topologically superimpose on half of a glucose molecule (Figure 2B) and may explain its relative success as an acceptor. In contrast, D-galactose, the epimer at position 4 of glucose, was a very bad acceptor (Figure 2A, spot *c'*). These data suggested that the topology of the hydroxyl group at position 4 might dramatically influence the acylation of the hydroxyl group at position 6, probably by steric effect (Figure 2B). In the presence of D-arabinose, the pentose unit found at the extremities of the cell wall arabinogalactan and carrying most of the mycoloyl chains in the outer membrane, a very weak signal was observed (Figure 2A, spot *f*). In the case of disaccharides, the yield of derivative biosynthesis was much lower with D-maltose [Glc(α 1→4)Glc] (Figure 2A, spot *a'*) than with trehalose [Glc(α,α 1→1)Glc] (spot *a*), underlining the importance of the nature of the glycosidic bond (Figure 2B). The signal obtained from D-cellobiose [Glc(β 1→4)Glc] (Figure 2A, spot *a''*) was even weaker than that observed with maltose, showing that a α anomery for the nonreducing glucose unit was favorable to the acyl transfer.

In conclusion, the FAAL32-Pks13 system has a narrow acceptor specificity: both the α-D-glucosyl motif and the (1→1) link between two glucose units compose the structural bases of an efficient transfer of the neosynthesized α-alkyl β-ketoacyl chains.

Prediction of a Trehalose-Binding Pocket in the TE$_{Pks13}$ Domain

We showed above that the FAAL32-Pks13 system itself catalyzes the release of its products. The fatty acyl-AMP ligase FAAL32 and the acyltransferase domain of Pks13 possess an acyltransferase activity, but they are dedicated to loading the acyl chain of both substrates onto Pks13 (Figure S1) (Gavalda et al., 2009; Léger et al., 2009). We hypothesized that the putative TE domain of Pks13 was responsible for the release step. The TE$_{Pks13}$ domain matched with α/β hydrolases of the

esterase-lipase superfamily, which cleave carboxylic (thio)ester bonds via a nucleophilic attack on the carbonyl. Structure-based sequence comparison of members of this family and programs for model quality evaluation validated the structure of the TE domain of the human fatty acid synthase (TE$_{hFAS}$) as the best template for homology modeling as well as the good quality of the resulting model (see Supplemental Experimental Procedures). The latter was performed using the structure of TE$_{hFAS}$ in complex with a polyunsaturated fatty acyl substrate analog (Protein Data Bank [PDB] ID 3TJM) (Zhang et al., 2011). The FAS catalyzes the biosynthesis of fatty acids via a Claisen condensation mechanism, a function closely related to that of Pks13. The TE$_{Pks13}$ model displayed a strict conservation of the catalytic triad (Ser1533, Asp1560, His1699 in the TE$_{Pks13}$ domain) (Figure 3A) and of the carboxyl(thio)esterase consensus sequence "G-X-S-X-G" holding the catalytic serine residue (Ser1533) responsible for the nucleophilic attack and the formation of a transient covalent link with the biosynthesis product. Furthermore, superimposition of the TE$_{Pks13}$ model with the TE$_{hFAS}$ structure revealed that the long groove-tunnel that accommodates the fatty acyl chain in TE$_{hFAS}$ domain (Zhang et al., 2011) was also present in TE$_{Pks13}$ model. Interestingly, unlike TE$_{hFAS}$, the TE$_{Pks13}$ predicted tunnel would open onto a large groove communicating with other grooves and tunnels and might potentially fit a very long fatty acyl chain (Figure S5). Enzymes of the Ag85ABC complex also belong to the α/β hydrolase family and catalyze the transfer of a mycoloyl chain onto a polyol core (the trehalose monomycolate), a function closely related to the mechanism of release of Pks13 products. To seek a putative trehalose-binding site in the TE$_{Pks13}$ domain, the model was compared with the crystal structure of Ag85B-trehalose complex (PDB ID 1F0P) (Anderson et al., 2001). Strikingly, the trehalose-binding pocket near the catalytic site in Ag85B (Figure 3C) superimposed well with a pocket at the bottom of the catalytic cavity in the TE$_{Pks13}$ domain, which might nicely accommodate the disaccharide (Figure 3B). In particular, two residues of Ag85B, the
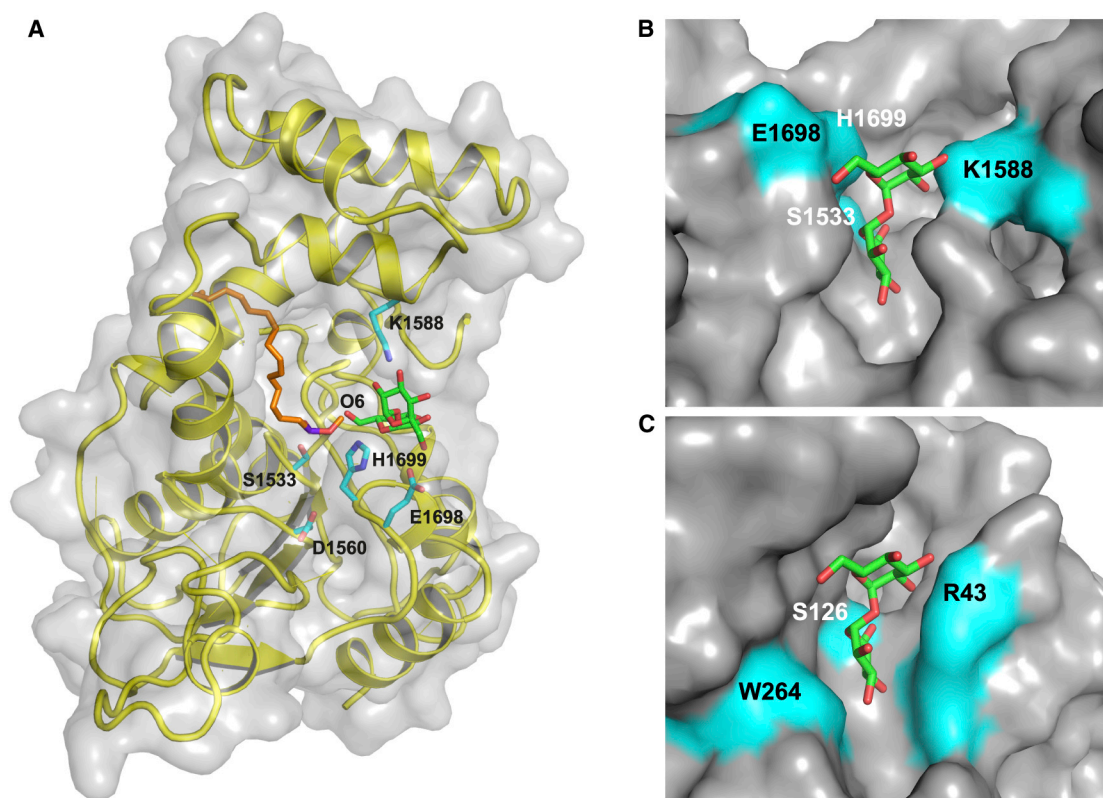
Figure 3. Homology Model of TE$_{Pks13}$ Domain and Its Predicted Trehalose-Binding Pocket

(A) Semi-transparent surface representation of the overall structure with the embedded backbone trace in yellow. The polyunsaturated ligand of the TE$_{hFAS}$ domain, methyl γ-linolenylfluorophosphonate, was positioned by superimposition of the model with the TE$_{hFAS}$ complex structure (PDB ID 3TJM) (Zhang et al., 2011) and drawn as orange sticks. The trehalose ligand of Ag85B enzyme was positioned by superimposition of the model with the Ag85B-trehalose complex structure (PDB ID 1F0P) (Anderson et al., 2001) and colored with carbon atoms in green. Residues of the catalytic triad, Ser1533, Asp1560, and His1699, as well as side chains of additional residues potentially interacting with trehalose (Lys1588 and Glu1698) are colored in cyan. Additional interactions might be mediated via water molecules and protein main chain atoms, as in the Ag85B-trehalose complex (Anderson et al., 2001). N, O, and P atoms are in blue, red, and purple, respectively.

(B) Surface representation of the predicted trehalose-binding pocket in the TE$_{Pks13}$ domain. Residues potentially interacting with trehalose are colored in cyan.

(C) Surface representation of the trehalose-binding pocket in the structure of the Ag85B-trehalose complex. Residues whose side chain directly interacts with trehalose are colored in cyan.

See also Figure S5.

catalytic Ser126 and Arg43, shown to directly interact with trehalose via their side chain, were conserved in the TE$_{Pks13}$ model (Ser1533 and Lys1588, respectively). The side chains of two additional residues of the TE$_{Pks13}$ domain, Glu1698 and the catalytic His1699, might also stabilize a trehalose ligand (Figures 3A and 3B). The hydroxyl group at position 6 of trehalose, where the acylation naturally occurs, would point toward the head group of the fatty acyl ligand, at an adequate distance for a transacylation reaction (Figure 3A).

Taken altogether, these data suggested that the TE$_{Pks13}$ domain was potentially active as a carboxyl(thio)esterase but that it might also be able to welcome a polyol-type molecule in its active site at a proper position for the transfer of an α-alkyl β-ketoacyl chain.

The Isolated TE$_{Pks13}$ Domain Exhibits an Acyltransferase Activity

To experimentally determine the function of TE$_{Pks13}$ domain, we designed an activity assay in the presence of the isolated domain and of a model substrate, palmitoyl-CoA (C_{16}-CoA), which holds a thioester bond between its acyl chain and the P-pant arm of the CoA moiety. We first validated the assay using the whole Pks13 in the presence of [1-^{14}C]C_{16}-CoA. The release of free C_{16} acid was strictly dependent upon the presence of Pks13 (Figure 4A, lane 3). In the presence of polyol, additional radiolabeled compounds appeared suggesting the formation of palmitoyl glucose (spot χ), trehalose (spots α and β), and glycerol (spot δ) derivatives (Figure 4A, lanes 4–7). Importantly, the synthesis of palmitic acid or polyol derivatives could not be detected using heat-inactivated Pks13 (Figure 4A, lane 2). Then, the TE$_{Pks13}$ domain was produced and purified to homogeneity from a recombinant *E. coli* strain (Figure S6). Similar to Pks13, incubation of the separate TE domain in the presence of [1-^{14}C]C_{16}-CoA induced the release of some C_{16} acid as shown by TLC and MS analysis (Figure 4B, lanes 4 and 7–10; Table S1). It also triggered the formation of additional compounds in the presence of molecules holding an α-D-glucose unit, namely trehalose, glucose, and maltose, as well as in the presence of glycerol (Figure 4B, lanes
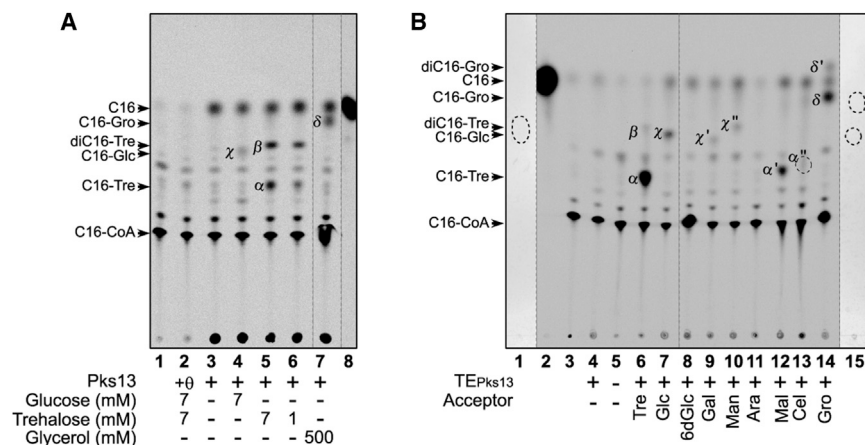
Figure 4. Thioesterase and Acyltransferase Activities of TE$_{Pks13}$ Domain

These activities were measured in the presence of a model substrate, [1-^{14}C]C$_{16}$-CoA, by TLC/phosphorimaging analysis. Representative data of three independent experiments. Eluent: Butan-1-ol/acetic acid/H$_2$O, 80/25/40. Spots: α, monopalmitoyl trehalose (C$_{16}$-Tre); α', palmitoyl maltose; α'', palmitoyl cellobiose; β, dipalmitoyl trehalose (diC$_{16}$-Tre); χ, palmitoyl glucose (C$_{16}$-Glc); χ', palmitoyl galactose; χ'', palmitoyl mannose; δ, palmitoyl glycerol (C$_{16}$-Gro); δ', dipalmitoyl glycerol (diC$_{16}$-Gro).

(A) Validation of the assay using the entire Pks13. Lane 1, [1-^{14}C]C$_{16}$-CoA standard; lanes 2–7, assays in the absence (−) or in the presence (+) of the mentioned putative acceptor molecule (at the indicated concentration); θ, heat-inactivated Pks13; lane 8, [1-^{14}C]C$_{16}$ acid standard.

(B) TE$_{Pks13}$ domain activity assays. Lane 1, diC$_{16}$-Tre standard; lane 2, [1-^{14}C]C$_{16}$ acid standard; lane 3, [1-^{14}C]C$_{16}$-CoA standard; lanes 4–14, assays in the absence (−) or in the presence (+) of the mentioned putative acceptor molecule (at 100 mM); lane 15, mix of C$_{16}$-Glc and C$_{16}$-Gro standards; 6dGlc, 6-deoxy-glucose. Cold standards were visualized by rhodamine B spraying and UV light.

See also Figure S6 and Table S1.

6, 7, 12, and 14). Consistently, MALDI-TOF spectra displayed the signals expected for the palmitoylated derivatives of these polyols (Table S1). In the presence of the other tested molecules (galactose, mannose, 6-deoxy-glucose, arabinose, and cellobiose), the activity of C$_{16}$ acyl transfer was very weak or undetectable (Figure 4B). Kinetic experiments performed with the TE$_{Pks13}$ domain determined an apparent K$_m$ for trehalose of 5.5 ± 0.1 mM, which was similar to values reported for trehalose-metabolizing enzymes (Kizawa et al., 1995; Riby and Galand, 1985). Consistent with Pks13's substrate specificity, the TE$_{Pks13}$ domain exhibited a marked predilection for trehalose as compared with glucose, with an apparent K$_m$ of 518 ± 30 mM for the latter. The very high K$_m$ value for glucose suggests that trehalose would be the specific acceptor of the neosynthesized α-alkyl β-ketoacyl chains in vivo.

In conclusion, the isolated TE domain of Pks13 is active and is able, like the entire Pks13 enzyme, to catalyze the transfer of a C$_{16}$ acyl chain from a P-pant arm onto trehalose.

The Transfer of Pks13 Condensation Products Is Catalyzed by Its Own TE Domain

To demonstrate the involvement of the TE domain in the transfer of the neosynthesized α-alkyl β-ketoacyl chains onto a polyol acceptor, the putative catalytic Ser1533 of Pks13 (Figure 3) was mutated into an Ala residue. Condensation assays for both wild-type (WT) Pks13 and Pks13 S1533A were performed in parallel in the presence of both trehalose and glycerol. Analysis of the intact samples revealed the lack of formation of α-alkyl β-ketoacid derivatives (TMMk and GroMMk) by Pks13 S1533A by comparison with WT Pks13 (Figure 5A, lanes 2 and 3). The lipid moiety of the condensation products was analyzed after chemical treatment (Figure 5C). A residual synthesis of condensation products (7%) by the mutant enzyme with respect to WT Pks13 was observed (Figure 5B, lanes 2 and 3). It most likely represented the α-alkyl β-ketoacyl chain that remained blocked on the C-terminal ACP domain (Figure S1) in the absence of an active TE domain. When some of the isolated WT TE$_{Pks13}$ domain

was added to the condensation assay with Pks13 S1533A, the acyltransferase function was recovered since some TMMk and GroMMk were synthesized (Figure 5A, lanes 4 and 5). In this case, the total condensation rate reached 18%–24% (Figure 5B, lanes 4 and 5). Thus, the WT TE$_{Pks13}$ domain was able to partially complement the S1533A mutation in the TE domain of the entire Pks13 enzyme.

These data altogether established that the TE$_{Pks13}$ domain is responsible for both the release and the transfer of Pks13 products onto a polyol acceptor molecule, particularly trehalose, and that S1533 is a key residue for this catalytic process (Figure S7). In the absence of an active TE domain, there is no catalytic turnover.

DISCUSSION

It is known that the ultimate biosynthesis steps of the mycolate-containing compounds are catalyzed by the mycoloyl transferases of the Ag85 complex. The latter transfers the mycoloyl chains from the TMM donor onto an acceptor, mainly arabinogalactan or another TMM but also glucose and possibly glycerol, to form the mAGP complex, TDM, GMM, and GroMM, which will reach their final locations in the mycomembrane (Figure 6) (Belisle et al., 1997; Jackson et al., 1999). However, the steps between the synthesis of the mycoloyl chains and the formation of TMM remained unknown, although they have been the subject of extensive investigations.

The present study allows elucidation of the missing steps and how to draw a scheme of the mycolate-containing compound biosynthesis (Figure 6). We have previously reported that after loading onto Pks13, the meromycolic and carboxyacyl chains are condensed via a Claisen-type mechanism by the ketosynthase domain of Pks13, resulting in a α-alkyl β-ketoacyl chain linked to the C-terminal ACP domain (Gavalda et al., 2009). Here we show that these highly insoluble mycolic acid precursors are not released as free acids in the bacterium by a classical hydrolysis step but are directly transferred onto a hydrophilic
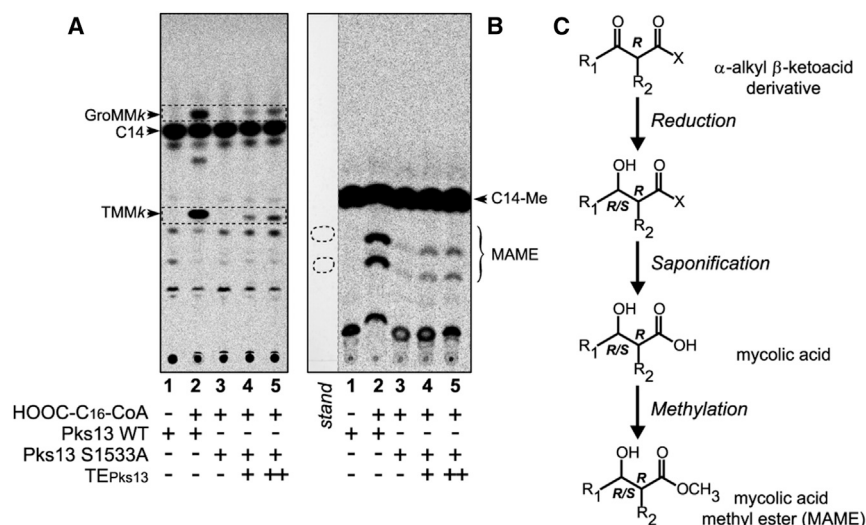
Figure 5. Condensation Assays Using Pks13 S1533A Enzyme

(A and B) TLC/phosphorimaging analyses. Representative data of three independent experiments. All assays were performed in the presence of trehalose and glycerol. Lanes 1, control assay without carboxy-C_{16}-CoA; lanes 2, assay with WT Pks13; lanes 3, assay with Pks13 S1533A; lanes 4, assay with Pks13 S1533A plus TE_{Pks13} domain; lanes 5, similar to lanes 4 with a double concentration of TE_{Pks13} domain (see Experimental Procedures); *stand*, cold standard of racemic mixture of C_{32} mycolic acid methyl esters (MAME), visualized by rhodamine B spraying and UV light.

(A) Intact reaction media. Eluent: $CHCl_3/CH_3OH/H_2O$, 65/25/4.

(B) Lipid moiety of the condensation products. Eluent: CH_2Cl_2.

(C) Chemical treatment of the condensation products for analysis of their lipid moiety. $R_1 = C_{13}$, $R_2 = C_{14}$, X = trehalose or glycerol (in assays 2, 4, and 5 in A and B) or Pks13 S1533A (in assay 3). For details, see Experimental Procedures.

See also Figure S7.

head, specifically trehalose (Figure S7). In conflict with the current biosynthesis model, our data demonstrate that their transfer is not performed by a discrete mycoloyl transferase as proposed earlier (Besra et al., 1994; Datta and Takayama, 1993; Takayama et al., 2005) but by Pks13's own TE domain. Thus, the latter releases the condensation products from the P-pant arm of the ACP domain, most likely via the formation of a transient ester bond with its catalytic Ser1533 residue (Figure S7; Figure 6). Then, the TE_{Pks13} domain catalyzes the cleavage of this bond and the concomitant transfer of the α-alkyl β-ketoacyl chain onto trehalose. The previous observations of an accumulation of α-alkyl β-ketoacyl trehalose in *cmrA* mycobacterial mutants deficient in the subsequent mycolic reductase step (Bhatt et al., 2008; Lea-Smith et al., 2007) are perfectly consistent with our data. After reduction by CmrA, the resulting TMM is translocated via MmpL3 transmembrane protein (Grzegorzewicz et al., 2012; Tahlan et al., 2012; Varela et al., 2012) toward the Ag85 complex tightly associated to the mycomembrane (Bou Raad et al., 2010; Marchand et al., 2012). The Ag85 enzymes then use TMM as a substrate for the biosynthesis of the mAGP complex and the mycolate-containing lipids located in the mycomembrane (Figure 6). LpqY-SugA-SugB-SugC ABC transporter mediates the retrograde transport of the extracellular released trehalose (Kalscheuer et al., 2010). This recycling step is critical for virulence of *M. tuberculosis* during the acute infection phase, which may be linked to the requirement of trehalose in the construction of the mycolic acid coat (Kalscheuer et al., 2010).

Similar to the mycolate-containing lipids, the biosynthesis of most lipid pathogenicity factors of the mycobacterial envelope depends upon the intervention of PKSs (Daffé et al., 2014; Jackson et al., 2007). For such molecules, data clearly outline an archetypal building and translocation pattern where fatty acyl chains are synthesized by specific PKSs, then transferred onto a polyol core, most often trehalose or substituted trehalose, and after potential extra modifications, the product is ultimately exported toward the envelope by a mycobacterial membrane

protein large (MmpL)-type transmembrane protein. This scheme is found for sulfolipid-1, polyacyl trehaloses, and lipooligosaccharides, whose fatty acyl chains are carried by a trehalose core, as well as for phenolic glycolipids and phthiocerol dimycocerosates, whose fatty acyl chains are carried by a phthiocerol core (Daffé et al., 2014). The present work combined with previous data highlight the conservation of this pattern for the mycolate-containing lipids (Figure 6). However, our data emphasize a fundamental discrepancy with the complex lipids cited above. For the latter, the PKS proteins involved do not contain any TE domain (Jackson et al., 2007) and the transacylation step is operated by discrete specific polyketide-associated protein (Pap)-type acyltransferases (Bhatt et al., 2007; Chavadi et al., 2012; Hatzios et al., 2009; Kumar et al., 2007; Onwueme et al., 2004; Rombouts et al., 2011). In contrast, there is no Pap-encoding gene in the vicinity of *pks13* gene on the chromosome (Cole et al., 1998). Instead, Pks13 is equipped with a TE domain structurally distinct from Pap enzymes, which is responsible for the transfer of the neosynthesized acyl chains onto the trehalose core, as discussed above. This unique mechanism of transfer of PKS products in mycobacteria appears as an extension of the macrocyclisation mechanism, catalyzed by many TE domains, where one nucleophilic atom of the polyketide plays the role of acceptor for the intramolecular transfer of the polyketide carbonyl extremity linked to the catalytic Ser (Frueh et al., 2008). In the case of TE_{Pks13}, the main difference resides in the fact that the transesterification is intermolecular and not intramolecular, and therefore the domain must adapt an acceptor molecule in its active site, close to the catalytic Ser (Figure S7). Accordingly, the presence of a hydrophilic pocket that might accommodate trehalose in the TE_{Pks13} domain active site, at an adequate distance for a transacylation reaction, was predicted by molecular modeling. Interestingly, an analogous intermolecular acyltransferase function has been recently reported for the PKS ArmB of the tree pathogen fungus *Armillaria mellea*. ArmB transfers its polyketide products onto a tricyclic sesquiterpene alcohol, generating a cytotoxic melleolide (Lackner et al., 2013), but the
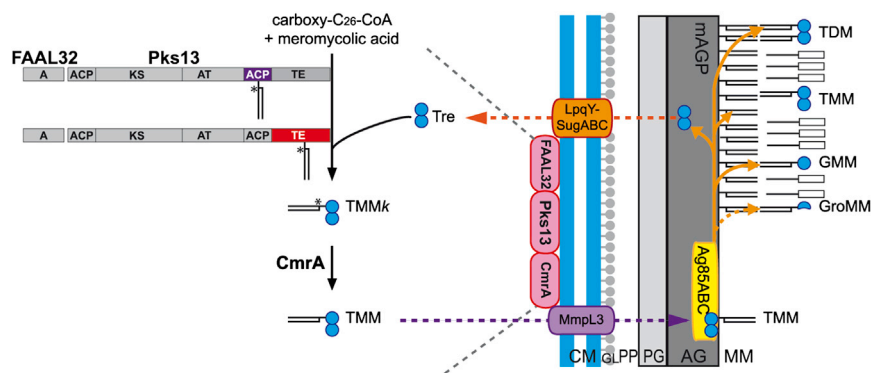
Figure 6. Proposed Schematic of the Last Steps of Mycolic Acid Biosynthesis and Transfer onto the Cell Wall in Mycobacteria

After loading onto Pks13, the acyl chains of carboxy-acyl-CoA and the meromycoloyl-AMP synthesized by FAAL32 are condensed by the enzyme resulting in an α-alkyl β-ketoacyl product linked through a thioester bond to the C-terminal ACP domain. The TE domain of Pks13 cleaves this bond and most likely forms a transient covalent ester bond between the α-alkyl β-ketoacyl chain and the catalytic Ser1533 in its active site. Then, the TE_{Pks13} domain transfers the condensation product onto trehalose to synthesize TMMk. This precursor is then reduced by CmrA into TMM. The latter is exported by MmpL3 membrane trans-porter, probably into the mycomembrane (MM), where it is used by the mycoloyltransferases (Ag85 complex) tightly associated to the mycomembrane to synthesize biologically active mycolate-containing compounds, i.e., the mAGP complex, the TDM, the GMM, and possibly the GroMM, which constitute major components of the mycomembrane. The released free trehalose is recycled by the LpqY-SugA-SugB-SugC ABC transporter. The scheme is inspired by the present study and previous works quoted in the text. CM, cytoplasmic membrane; GL, granular layer; PP, periplasm; PG, peptidoglycan; AG, arabinogalactan; MM, mycomembrane; *, keto function.
See also Figure S1.

involvement of its TE domain in this step has not been demonstrated yet.

The mycolic acid biosynthesis is the target of the TB drugs isoniazid, ethionamide, and thiacetazone. Furthermore, most of the newly discovered molecules showing promise for the treatment of TB, notably multidrug-resistant TB, inhibit aspects of *M. tuberculosis* cell envelope biogenesis, including the mycolate-containing compound metabolism (Jackson et al., 2013). In particular, target-based screenings focusing on this pathway were successful (North et al., 2014). Given its unique features, the TE_{Pks13} domain constitutes an attractive target for drug development. The recent discovery of a benzofuran molecule both targeting the TE_{Pks13} domain and inhibiting *M. tuberculosis* growth validates this domain as a vulnerable and druggable target (Ioerger et al., 2013). The activity assays with the isolated TE domain and the entire Pks13 enzyme designed during the present work constitute precious tools that we are currently using for the screening of putative anti-TB molecules.

SIGNIFICANCE

The envelope of the tubercle bacillus contains critical pathogenicity factors made of exotic very long chain fatty acids carried by a polyol core. So far, the archetypal building pattern of these complex lipids corresponded to the biosynthesis of the fatty acyl chains by specific polyketide synthases, followed by their transfer onto the polyol moiety catalyzed by a discrete Pap-type acyltransferase. In the specific case of the mycolate-containing compounds, we have previously shown that Pks13 polyketide synthase catalyzes the condensation reaction that produces α-alkyl β-ketoacyl chains, direct precursors of the mycolates (Gavalda et al., 2009). However, the enzymes/domains responsible for the release of the condensation products from Pks13 and for their transfer onto a polyol core remain unknown, leaving gaps in the knowledge of the mycolate-containing compound biosynthesis pathway. In contrast to the current

biosynthesis model suggesting the involvement of a discrete mycoloyl transferase, the present work shows that Pks13 catalyzes itself the cleavage of the thioester bond between the enzyme and the neosynthesized acyl chains. We demonstrate that this function is carried by its thioesterase-like (TE_{Pks13}) domain. Most importantly, the latter exhibits an acyltransferase function and directly transfers the mycolate precursors onto a specific polyol acceptor molecule, trehalose, ultimately leading to the formation of trehalose monomycolate, a common precursor of the mycolate-containing compounds. Thus, the lipid transfer mechanism involved does not use the conventional Pap-type acyltransferases, in conflict with the archetypal biosynthesis pattern of the mycobacterial complex lipids. Whole-cell screening on *M. tuberculosis* has recently shown that the unique TE domain of Pks13 represents a vulnerable and attractive target for drug development to cure tuberculosis (Ioerger et al., 2013).

EXPERIMENTAL PROCEDURES

Protein Production and Purification
See Supplemental Experimental Procedures.

Enzymatic Assays
Condensation assays contained 40 μM [1-^{14}C]C$_{14}$ acid (specific activity: 54 mCi/mmol, American Radiolabeled Chemicals) and 40 μM carboxy-C$_{16}$-CoA (synthesized and purified as described previously [Gavalda et al., 2009]), 8 mM MgCl$_2$, and 2 mM ATP, in 50 mM HEPES (pH 7.2). The reactions (total volume: 10 μl) were started by the addition of 1–2 μM FAAL32 and 2 μM Pks13, incubated for 6 hr at 30°C, then stopped at −20°C. Control experiments without certain reagents or using heat-inactivated Pks13 (heated 10 min at 95°C) were performed, as mentioned in the text or figure legends. For MS analyses, condensation assays were run in the same conditions with cold substrates, in 100 μl final volume. The effect of putative acceptor molecules was evaluated by adding them at various concentrations, as mentioned in the text or figure legends, in the presence of enzymes from glycerol-free stocks. In vitro complementation assays were performed in the presence of 200 mM trehalose and 500 mM glycerol, 1 μM FAAL32, and 1 μM of either WT Pks13 or Pks13 S1533A, ±4 or 8 μM of purified TE_{Pks13} domain. The reaction media were either kept intact or submitted to the following treatment: samples were mixed with

100 μl tetrahydrofuran and reduced for 1 hr by adding 500 μl NaBH$_4$ 0.5 M in ethanol 99%; reactions were stopped by addition of 1 ml acetic acid; for saponification, 1.5 ml KOH 10% (w/v) in CH$_3$OH:toluene, 8:2 were added and samples incubated for 1 hr at 80°C; the media were then acidified with 2 ml H$_2$SO$_4$; and lipids were extracted with diethylether, washed with water, dried, and methylated with diazomethane (Figure 5C). Thioesterase and acyltransferase activity assays were performed with either 40 μM [1-^{14}C]C$_{16}$-CoA (specific activity: 60 mCi/mmol, Perkin Elmer) or cold C$_{16}$-CoA (for MS analysis), 100 mM (for TE$_{Pks13}$ assays) or variable concentrations (for Pks13; specified in Figure 4) of putative acceptor, and either 2 μM Pks13 or 4 μM TE$_{Pks13}$ domain, in 50 mM HEPES (pH 7.2), incubated for 6 hr at 30°C, then frozen at –20°C. For all assays, the solvent coming from the substrate solutions was evaporated before addition of the other reagents. All assays were performed at least in three independent experiments. K$_m$ were measured in the presence of TE$_{Pks13}$ (2 μM), a fixed concentration of [1-^{14}C]C$_{16}$-CoA (40 μM), and variable concentrations of trehalose (0.01–200 mM) or glucose (0.5–1000 mM; higher concentrations could not be used because of problems of solubility and migration on thin layer). The experimental conditions were selected in order to be in a linear response range. Data were fitted to the Michaelis-Menten equation by least-squares fits to a hyperbola using the program GraphPad Prism version 5.04.

TLC Analyses
See also Supplemental Experimental Procedures. Intact media of condensation assays and thioesterase/transacylase activity assays were analyzed by TLC on silica gel G60 plates developed with CHCl$_3$/CH$_3$OH/H$_2$O 65/25/4 and butan-1-ol/acetic acid/water 80/25/40, respectively. The lipid extracts from reaction media or purified compounds submitted to chemical treatment were spotted on TLC plates as diethylether solutions and developed with dichloromethane. The radiolabeling was detected by phosphorimaging (Variable Mode Imager Typhoon TRIO, Amersham Biosciences) and quantified in arbitrary units using the ImageQuant version 5.1 software (Molecular Dynamics).

MALDI-TOF MS and MS/MS
See Supplemental Experimental Procedures.

Homology Modeling, Structural Comparison, and Visualization
See details in Supplemental Experimental Procedures. The SWISS-MODEL program (www.swissmodel.expasy.org) (Arnold et al., 2006) was used to generate a homology model from the sequence of the TE$_{Pks13}$ domain. Structure visualization and analyses were carried out using the PyMOL program (www.pymol.org).

SUPPLEMENTAL INFORMATION

Supplemental Information includes Supplemental Experimental Procedures, seven figures, and one table and can be found with this article online at http://dx.doi.org/10.1016/j.chembiol.2014.10.011.

AUTHOR CONTRIBUTIONS

S.G., F.B., L.M., and A.Q. conceived and designed experiments; S.G., F.B., F.L., L.M., and A.Q. performed research; S.G. and F.B. performed radiolabeled activity assays, competition experiments, and TLC/phosphorimaging analyses; S.G. made all chemical treatments of reaction products; F.B. performed cold activity assays for MALDI-TOF MS analysis and TE$_{Pks13}$ kinetic experiments; F.L., C.B., W.M., C.C., and C.G. contributed to reagents, material, or analysis tools; S.G., F.B., F.L., L.M., M.D., and A.Q. analyzed data; M.D. and A.Q. supervised the project; S.G., L.M., and A.Q. created the figures; and A.Q. wrote the paper. Most authors commented or contributed to sections of the manuscript.

REFERENCES

Anderson, D.H., Harth, G., Horwitz, M.A., and Eisenberg, D. (2001). An interfacial mechanism and a class of inhibitors inferred from two crystal structures of the *Mycobacterium tuberculosis* 30 kDa major secretory protein (Antigen 85B), a mycolyl transferase. J. Mol. Biol. *307*, 671–681.

Arnold, K., Bordoli, L., Kopp, J., and Schwede, T. (2006). The SWISS-MODEL workspace: a web-based environment for protein structure homology modelling. Bioinformatics *22*, 195–201.

Belisle, J.T., Vissa, V.D., Sievert, T., Takayama, K., Brennan, P.J., and Besra, G.S. (1997). Role of the major antigen of *Mycobacterium tuberculosis* in cell wall biogenesis. Science *276*, 1420–1422.

Besra, G.S., Sievert, T., Lee, R.E., Slayden, R.A., Brennan, P.J., and Takayama, K. (1994). Identification of the apparent carrier in mycolic acid synthesis. Proc. Natl. Acad. Sci. USA *91*, 12735–12739.

Bhatt, K., Gurcha, S.S., Bhatt, A., Besra, G.S., and Jacobs, W.R., Jr. (2007). Two polyketide-synthase-associated acyltransferases are required for sulfolipid biosynthesis in *Mycobacterium tuberculosis*. Microbiology *153*, 513–520.

Bhatt, A., Brown, A.K., Singh, A., Minnikin, D.E., and Besra, G.S. (2008). Loss of a mycobacterial gene encoding a reductase leads to an altered cell wall containing beta-oxo-mycolic acid analogs and accumulation of ketones. Chem. Biol. *15*, 930–939.

Bou Raad, R., Méniche, X., de Sousa-d'Auria, C., Chami, M., Salmeron, C., Tropis, M., Labarre, C., Daffé, M., Houssin, C., and Bayan, N. (2010). A deficiency in arabinogalactan biosynthesis affects *Corynebacterium glutamicum* mycolate outer membrane stability. J. Bacteriol. *192*, 2691–2700.

Chavadi, S.S., Onwueme, K.C., Edupuganti, U.R., Jerome, J., Chatterjee, D., Soll, C.E., and Quadri, L.E. (2012). The mycobacterial acyltransferase PapA5 is required for biosynthesis of cell wall-associated phenolic glycolipids. Microbiology *158*, 1379–1387.

Cole, S.T., Brosch, R., Parkhill, J., Garnier, T., Churcher, C., Harris, D., Gordon, S.V., Eiglmeier, K., Gas, S., Barry, C.E., 3rd., et al. (1998). Deciphering the biology of *Mycobacterium tuberculosis* from the complete genome sequence. Nature *393*, 537–544.

Daffé, M., Crick, D.C., and Jackson, M. (2014). Genetics of capsular polysaccharides and cell envelope (glyco)lipids. In Molecular Genetics of Mycobacteria, G.F. Hatfull and W.R. Jacobs, Jr., eds. (Washington, DC: ASM Press), pp. 559–609.

Datta, A.K., and Takayama, K. (1993). Biosynthesis of a novel 3-oxo-2-tetradecyloctadecanoate-containing phospholipid by a cell-free extract of *Corynebacterium diphtheriae*. Biochim. Biophys. Acta *1169*, 135–145.

Esin, S., Counoupas, C., Aulicino, A., Brancatisano, F.L., Maisetta, G., Bottai, D., Di Luca, M., Florio, W., Campa, M., and Batoni, G. (2013). Interaction of *Mycobacterium tuberculosis* cell wall components with the human natural killer cell receptors NKp44 and Toll-like receptor 2. Scand. J. Immunol. *77*, 460–469.

Frueh, D.P., Arthanari, H., Koglin, A., Vosburg, D.A., Bennett, A.E., Walsh, C.T., and Wagner, G. (2008). Dynamic thiolation-thioesterase structure of a nonribosomal peptide synthetase. Nature *454*, 903–906.

Gavalda, S., Léger, M., van der Rest, B., Stella, A., Bardou, F., Montrozier, H., Chalut, C., Burlet-Schiltz, O., Marrakchi, H., Daffé, M., and Quémard, A. (2009). The Pks13/FadD32 crosstalk for the biosynthesis of mycolic acids in *Mycobacterium tuberculosis*. J. Biol. Chem. *284*, 19255–19264.

Gebhardt, H., Meniche, X., Tropis, M., Krämer, R., Daffé, M., and Morbach, S. (2007). The key role of the mycolic acid content in the functionality of the cell wall permeability barrier in Corynebacterineae. Microbiology *153*, 1424–1434.

Geisel, R.E., Sakamoto, K., Russell, D.G., and Rhoades, E.R. (2005). In vivo activity of released cell wall lipids of *Mycobacterium bovis* bacillus Calmette-Guérin is due principally to trehalose mycolates. J. Immunol. *174*, 5007–5015.

Glickman, M.S. (2008). Cording, cord factors, and trehalose dimycolate. In The Mycobacterial Cell Envelope, M. Daffé and J.M. Reyrat, eds. (Washington, DC: ASM Press), pp. 63–73.

Grzegorzewicz, A.E., Pham, H., Gundi, V.A., Scherman, M.S., North, E.J., Hess, T., Jones, V., Gruppo, V., Born, S.E., Korduláková, J., et al. (2012). Inhibition of mycolic acid transport across the *Mycobacterium tuberculosis* plasma membrane. Nat. Chem. Biol. *8*, 334–341.

Hatzios, S.K., Schelle, M.W., Holsclaw, C.M., Behrens, C.R., Botyanszki, Z., Lin, F.L., Carlson, B.L., Kumar, P., Leary, J.A., and Bertozzi, C.R. (2009). PapA3 is an acyltransferase required for polyacyltrehalose biosynthesis in *Mycobacterium tuberculosis*. J. Biol. Chem. *284*, 12745–12751.

Hertweck, C. (2009). The biosynthetic logic of polyketide diversity. Angew. Chem. Int. Ed. Engl. *48*, 4688–4716.

Ioerger, T.R., O'Malley, T., Liao, R., Guinn, K.M., Hickey, M.J., Mohaideen, N., Murphy, K.C., Boshoff, H.I., Mizrahi, V., Rubin, E.J., et al. (2013). Identification of new drug targets and resistance mechanisms in *Mycobacterium tuberculosis*. PLoS ONE *8*, e75245.

Jackson, M., Raynaud, C., Lanéelle, M.A., Guilhot, C., Laurent-Winter, C., Ensergueix, D., Gicquel, B., and Daffé, M. (1999). Inactivation of the antigen 85C gene profoundly affects the mycolate content and alters the permeability of the *Mycobacterium tuberculosis* cell envelope. Mol. Microbiol. *31*, 1573–1587.

Jackson, M., Stadthagen, G., and Gicquel, B. (2007). Long-chain multiple methyl-branched fatty acid-containing lipids of *Mycobacterium tuberculosis*: biosynthesis, transport, regulation and biological activities. Tuberculosis (Edinb.) *87*, 78–86.

Jackson, M., McNeil, M.R., and Brennan, P.J. (2013). Progress in targeting cell envelope biogenesis in *Mycobacterium tuberculosis*. Future Microbiol. *8*, 855–875.

Kalscheuer, R., Weinrick, B., Veeraraghavan, U., Besra, G.S., and Jacobs, W.R., Jr. (2010). Trehalose-recycling ABC transporter LpqY-SugA-SugB-SugC is essential for virulence of *Mycobacterium tuberculosis*. Proc. Natl. Acad. Sci. USA *107*, 21761–21766.

Kizawa, H., Miyagawa, K., and Sugiyama, Y. (1995). Purification and characterization of trehalose phosphorylase from *Micrococcus varians*. Biosci. Biotechnol. Biochem. *59*, 1908–1912.

Koglin, A., and Walsh, C.T. (2009). Structural insights into nonribosomal peptide enzymatic assembly lines. Nat. Prod. Rep. *26*, 987–1000.

Kumar, P., Schelle, M.W., Jain, M., Lin, F.L., Petzold, C.J., Leavell, M.D., Leary, J.A., Cox, J.S., and Bertozzi, C.R. (2007). PapA1 and PapA2 are acyltransferases essential for the biosynthesis of the *Mycobacterium tuberculosis* virulence factor sulfolipid-1. Proc. Natl. Acad. Sci. USA *104*, 11221–11226.

Lackner, G., Bohnert, M., Wick, J., and Hoffmeister, D. (2013). Assembly of melleolide antibiotics involves a polyketide synthase with cross-coupling activity. Chem. Biol. *20*, 1101–1106.

Layre, E., Collmann, A., Bastian, M., Mariotti, S., Czaplicki, J., Prandi, J., Mori, L., Stenger, S., De Libero, G., Puzo, G., and Gilleron, M. (2009). Mycolic acids constitute a scaffold for mycobacterial lipid antigens stimulating CD1-restricted T cells. Chem. Biol. *16*, 82–92.

Lea-Smith, D.J., Pyke, J.S., Tull, D., McConville, M.J., Coppel, R.L., and Crellin, P.K. (2007). The reductase that catalyzes mycolic motif synthesis is required for efficient attachment of mycolic acids to arabinogalactan. J. Biol. Chem. *282*, 11000–11008.

Léger, M., Gavalda, S., Guillet, V., van der Rest, B., Slama, N., Montrozier, H., Mourey, L., Quémard, A., Daffé, M., and Marrakchi, H. (2009). The dual function of the *Mycobacterium tuberculosis* FadD32 required for mycolic acid biosynthesis. Chem. Biol. *16*, 510–519.

Marchand, C.H., Salmeron, C., Bou Raad, R., Méniche, X., Chami, M., Masi, M., Blanot, D., Daffé, M., Tropis, M., Huc, E., et al. (2012). Biochemical disclosure of the mycolate outer membrane of *Corynebacterium glutamicum*. J. Bacteriol. *194*, 587–597.

Marrakchi, H., Lanéelle, M.A., and Daffé, M. (2014). Mycolic acids: structures, biosynthesis, and beyond. Chem. Biol. *21*, 67–85.

Moody, D.B., Briken, V., Cheng, T.Y., Roura-Mir, C., Guy, M.R., Geho, D.H., Tykocinski, M.L., Besra, G.S., and Porcelli, S.A. (2002). Lipid length controls antigen entry into endosomal and nonendosomal pathways for CD1b presentation. Nat. Immunol. *3*, 435–442.

North, E.J., Jackson, M., and Lee, R.E. (2014). New approaches to target the mycolic acid biosynthesis pathway for the development of tuberculosis therapeutics. Curr. Pharm. Des. *20*, 4357–4378.

Onwueme, K.C., Ferreras, J.A., Buglino, J., Lima, C.D., and Quadri, L.E. (2004). Mycobacterial polyketide-associated proteins are acyltransferases: proof of principle with *Mycobacterium tuberculosis* PapA5. Proc. Natl. Acad. Sci. USA *101*, 4608–4613.

Portevin, D., De Sousa-D'Auria, C., Houssin, C., Grimaldi, C., Chami, M., Daffé, M., and Guilhot, C. (2004). A polyketide synthase catalyzes the last condensation step of mycolic acid biosynthesis in mycobacteria and related organisms. Proc. Natl. Acad. Sci. USA *101*, 314–319.

Promé, J.C., Walker, R.W., and Lacave, C. (1974). Condensation de deux molécules d'acide palmitique chez *Corynebacterium diphtheriae*: formation d'un béta-céto-ester de tréhalose. C. R. Acad. Sci. *278*, 1065–1068.

Puzo, G., Tissié, G., Aurelle, H., Lacave, C., and Promé, J.C. (1979). Occurrence of 3-oxo-acyl groups in the 6,6′-diesters of alpha-D-trehalose. New glycolipids related to cord factor from *Corynebacterium diphtheriae*. Eur. J. Biochem. *98*, 99–105.

Riby, J., and Galand, G. (1985). Rat intestinal brush border membrane trehalase: some properties of the purified enzyme. Comp. Biochem. Physiol. B *82*, 821–827.

Rombouts, Y., Alibaud, L., Carrère-Kremer, S., Maes, E., Tokarski, C., Elass, E., Kremer, L., and Guérardel, Y. (2011). Fatty acyl chains of *Mycobacterium marinum* lipooligosaccharides: structure, localization and acylation by PapA4 (MMAR_2343) protein. J. Biol. Chem. *286*, 33678–33688.

Shimakata, T., Tsubokura, K., and Kusaka, T. (1986). Requirement of glucose for mycolic acid biosynthetic activity localized in the cell wall of *Bacterionema matruchotii*. Arch. Biochem. Biophys. *247*, 302–311.

Tahlan, K., Wilson, R., Kastrinsky, D.B., Arora, K., Nair, V., Fischer, E., Barnes, S.W., Walker, J.R., Alland, D., Barry, C.E., 3rd, and Boshoff, H.I. (2012). SQ109 targets MmpL3, a membrane transporter of trehalose monomycolate involved in mycolic acid donation to the cell wall core of *Mycobacterium tuberculosis*. Antimicrob. Agents Chemother. *56*, 1797–1809.

Takayama, K., Wang, C., and Besra, G.S. (2005). Pathway to synthesis and processing of mycolic acids in *Mycobacterium tuberculosis*. Clin. Microbiol. Rev. *18*, 81–101.

Tropis, M., Meniche, X., Wolf, A., Gebhardt, H., Strelkov, S., Chami, M., Schomburg, D., Krämer, R., Morbach, S., and Daffé, M. (2005). The crucial role of trehalose and structurally related oligosaccharides in the biosynthesis and transfer of mycolic acids in Corynebacterineae. J. Biol. Chem. *280*, 26573–26585.

Varela, C., Rittmann, D., Singh, A., Krumbach, K., Bhatt, K., Eggeling, L., Besra, G.S., and Bhatt, A. (2012). MmpL genes are associated with mycolic acid metabolism in mycobacteria and corynebacteria. Chem. Biol. *19*, 498–506.

Vilchèze, C., Morbidoni, H.R., Weisbrod, T.R., Iwamoto, H., Kuo, M., Sacchettini, J.C., and Jacobs, W.R., Jr. (2000). Inactivation of the inhA-encoded fatty acid synthase II (FASII) enoyl-acyl carrier protein reductase induces accumulation of the FAS end products and cell lysis of *Mycobacterium smegmatis*. J. Bacteriol. *182*, 4059–4067.

Walsh, C.T., Gehring, A.M., Weinreb, P.H., Quadri, L.E., and Flugel, R.S. (1997). Post-translational modification of polyketide and nonribosomal peptide synthases. Curr. Opin. Chem. Biol. *1*, 309–315.

WHO (2013). Global tuberculosis report 2013. (Geneva: WHO Press).

Zhang, W., Chakravarty, B., Zheng, F., Gu, Z., Wu, H., Mao, J., Wakil, S.J., and Quiocho, F.A. (2011). Crystal structure of FAS thioesterase domain with polyunsaturated fatty acyl adduct and inhibition by dihomo-gamma-linolenic acid. Proc. Natl. Acad. Sci. USA *108*, 15757–15762.